

# Background reduction and systematic uncertainty of the ESD method in the OPERA experiment

T. Hayakawa

December 16, 2022

## Abstract

This is a supplementary material for the paper “Updated constraints on sterile neutrino mixing in the OPERA experiment using a new  $\nu_e$  identification method” [1].

## 1 Background reduction

In the ESD method, the background sources shown in Figure 1 are considered: (1)  $e^+e^-$  pairs produced by prompt conversion of  $\gamma$ -rays from  $\pi^0$  decays before the vertex film<sup>1</sup>, (2) random coincidence of a hadron track and  $\gamma$ -ray conversion, and (3)  $\tau \rightarrow e$  decay from  $\nu_\tau$  CC interaction. (3) is mostly eliminated by the  $\nu_\tau$  identification described in [2]. On the contrary, large number of (1) and (2) backgrounds are expected to be detected due to the high detection efficiency for the electromagnetic (e.m.) showers of the ESD method. If all  $0\mu$  events are completely analyzed and no background reduction methods are applied, the expected number of (1) and (2) are  $64 \pm 11$  and  $115 \pm 18$ . They are significantly larger than the expected  $\nu_e$  CC interactions, which are  $6.3 \pm 0.6$  in absence of background reduction methods.

### 1.1 Prompt $\gamma$ conversion

In most cases, the prompt  $\gamma$  conversion (1) leaves a pair of almost parallel tracks by  $e^+e^-$  on the vertex film. The submicron spatial resolution of emulsion films can detect each of them separately. Therefore the number of tracks around the primary electron candidates are the most important information to distinguish the  $\nu_e$  CC interactions from the prompt  $\gamma$  conversions. In the vertex film, many hadron and electron tracks not originated from the primary electron or  $\gamma$ -rays are recorded. To remove them, the pair track candidates are selected by the following criteria.

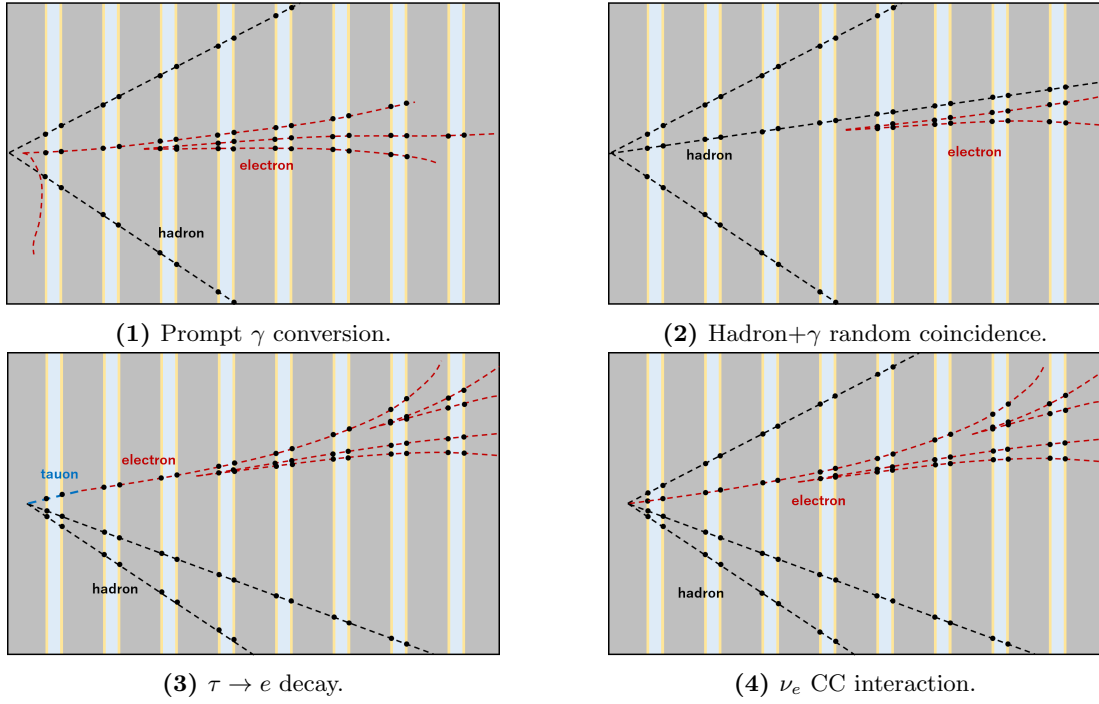
1. within  $70 \mu\text{m}$  and  $0.3 \text{ rad}$  from the primary electron candidate.
2. consisting of less than 8 track segments or e.m. showers.

Figure 2 shows the distributions of the distance and the angular difference from the primary electron and the cut above.

---

<sup>1</sup>The film immediately downstream of the neutrino interaction vertex.





**Figure 1:** Three background sources from (1) prompt  $\gamma$  conversion, (2) hadron+ $\gamma$  random coincidence, (3)  $\tau \rightarrow e$  decay, and (4)  $\nu_e$  CC interaction.

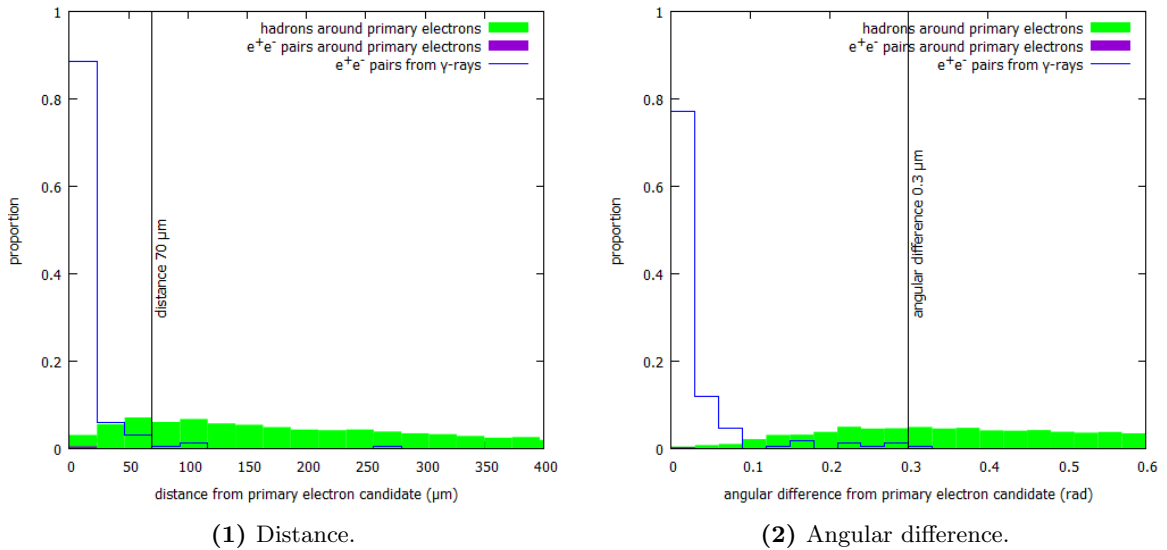


**Figure 2:** Distributions of (1) the distance and (2) the angular difference from the primary electron candidate.

In addition, the energy of e.m. showers are also useful for the classification of  $\nu_e$  CC interactions. The energy reconstruction of e.m. showers is performed by a neural-network-based method using e.m. shower properties: direction of the primary electron, track position and angular distributions from the primary electrons in each film. The e.m. shower energy on MC simulation versus its reconstructed energy is shown in Figure 3. The energy reconstruction accuracy is about 34%. The reconstructed energies tend to be smaller than the true ones above  $> 10$  GeV, and it is considered to be due to the energy leak of e.m. showers outside from the scanning area of 20 films. However the energy accuracy of the high energy e.m. showers is not critical and would not have an impact to the background reduction.

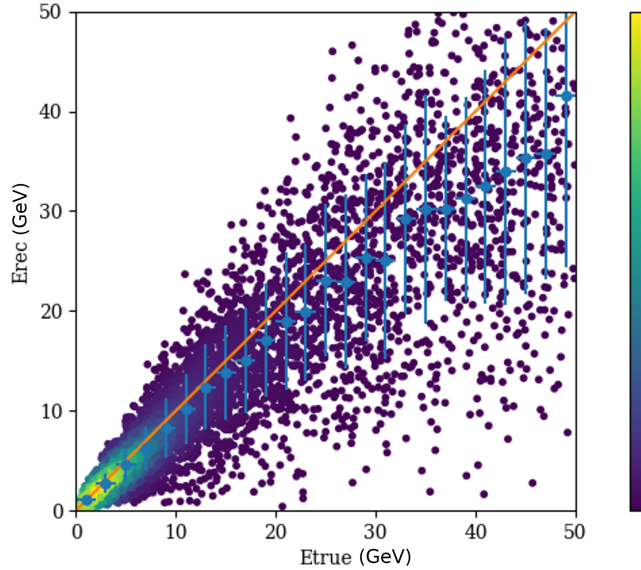


**Figure 3:** MC truth vs reconstructed energy of e.m. showers.

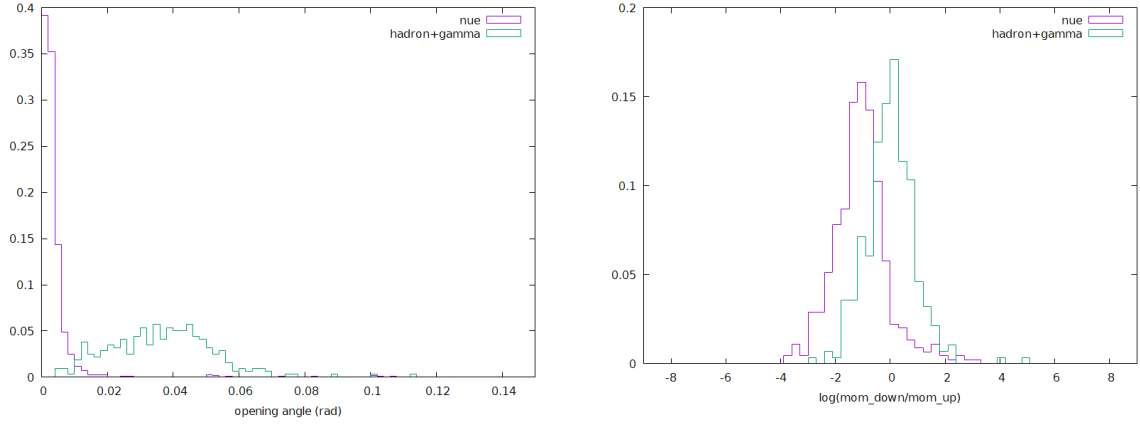
Events that have even number of electron-like tracks<sup>2</sup> including the primary electron candidate or have a reconstructed energy of less than 1.1 GeV are classified as prompt  $\gamma$  conversion. The expected number of this background decreases to  $2.1 \pm 0.7$ , while the loss of  $\nu_e$  CC interaction events is about 8%. The selection criteria have been optimized to maximize the statistical significance of  $\nu_e$  appearance.

## 1.2 Hadron + $\gamma$ random coincidence

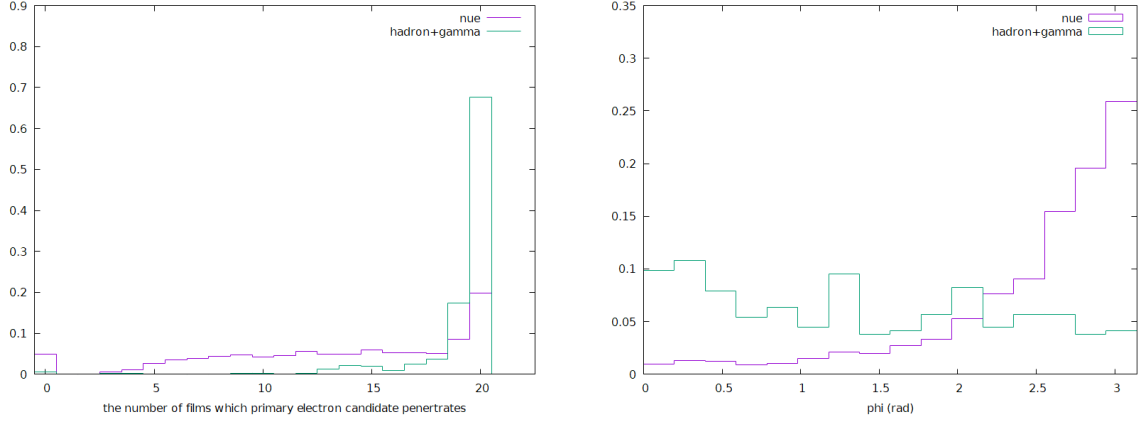
The hadron +  $\gamma$  random coincidence is defined as an overlap of hadrons and e.m. showers inside a shower detection cone. Most of these events are removed by using minimum opening angles between the primary electron candidates and all  $e^+e^-$  pairs' directions ( $\theta$ ), however, non-negligible amount of these events remain. To achieve a sufficient signal-to-noise ratio, a maximum likelihood estimation with 3 additional variables is introduced: ratio of the momentum of the primary electron candidate measured in the 1st-9th plates relative to the 10th-18th plates from the most upstream film ( $q$ ), number of films which the primary electron candidate penetrates ( $s$ ), mean azimuthal opening angle between the primary electron candidate and the

<sup>2</sup>The primary electron candidate, or tracks not removed by the pair track selection above.

hadrons ( $\phi$ ). In Figure 4, the distributions of these variables of the  $\nu_e$  CC interactions obtained by the MC simulation are compared to those of the hadron +  $\gamma$  random coincidences. The likelihood function for  $i = \nu_e, h + \gamma$  is defined as:



( $\theta$ ) minimum opening angle between the primary ( $q$ ) ratio of the momentum of the primary electron candidate and all  $e^+e^-$  pairs' directions. electron candidate measured in the 1st-9th plates relative to the 10th-18th plates from the most upstream film.



( $s$ ) number of films which the primary electron candidate penetrates. ( $\phi$ ) mean azimuthal opening angle between the primary electron candidate and the hadrons.

**Figure 4:** The distributions of the variables used in the maximum likelihood estimation.

$$L^i(q, s, \phi, \theta) = QS^i(q, s) \cdot \Phi^i(\phi) \cdot \Theta^i(\theta) \quad (1)$$

where  $\Phi^i(\phi)$  and  $\Theta^i(\theta)$  are the probability density functions of  $\phi$  and  $\theta$ .  $QS^i(q, s)$  is defined as:

$$QS^i(q, s) = \begin{cases} Q^i(q) (1 - S^i) & \text{if } s \geq 18 \\ S^i & \text{if } s < 18 \end{cases} \quad (2)$$

$Q^i(q)$  is also a probability density function of  $q$ .  $S^i$  is the probability that the primary electron candidate of  $i$  stops before penetrating 18 films, and estimated as  $S^{\nu_e} = 0.665$ ,  $S^{h+\gamma} =$

0.111 by the MC simulation. From the above, we define a reliability function  $R(q, s, \phi, \theta)$  by a log-likelihood ratio.

$$R(q, s, \phi, \theta) = \log \frac{L^{\nu_e}(q, s, \phi, \theta)}{L^{h+\gamma}(q, s, \phi, \theta)} \quad (3)$$

Events with the value of  $R$  less than 0 are classified as hadron+ $\gamma$  random coincidence and removed from the  $\nu_e$  CC interaction candidates. Figure 5 shows the distribution of the function  $R$ . After this selection, remaining backgrounds are estimated to be only  $1.2 \pm 0.5$  and the loss of  $\nu_e$  CC interactions is estimated to be 2%.

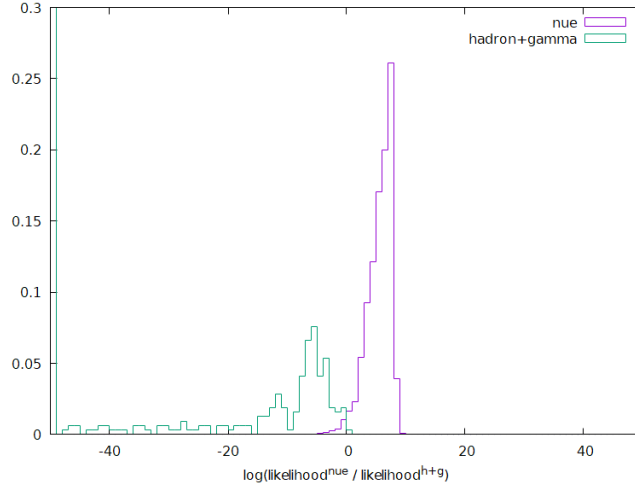


**Figure 5:** The distribution of the reliability function.

### 1.3 Comparison to data

Here we compare the expected number of events rejected by the methods to the data. In the paper, a sample of 99 events interacting at the most upstream part of ECCs are selected as the target for the ESD method. The expected number of the background events are estimated by the MC simulation including the sub-sample selection and the normalization described in the paper. Table 1 shows those of both background sources. The “Rejected” column means the number of observed events classified as non  $\nu_e$  candidate by the background reduction methods described above. The MC expectation and observed data are consistent.

## 2 Systematic uncertainty

The systematic uncertainty for the CSH method was conservatively estimated to be 20%/10% for the  $\nu_e$  energies below/above 10 GeV [3]. It should be noted that the CSH and ESD methods have common systematic uncertainties of the CNGS flux, cross section and location procedure, comprehensively estimated to be 14%/6% for energies below/above 10 GeV. The uncertainty

<sup>3</sup>Since no additional selection for the backgrounds from  $\tau \rightarrow e$  decays are introduced, this number is the same as that of the “After BG cut” column.

E.m. shower source	Observed		MC simulation	
	Rejected	$\nu_e$ cand	No BG cut	After BG cut
prompt $\gamma$ conversion	4	-	$5.3 \pm 1.2$	$0.3 \pm 0.1$
h+ $\gamma$ random coincidence	12	-	$12.0 \pm 2.3$	$0.1 \pm 0.1$
$\tau \rightarrow e$ decay	0	-	$0.05 \pm 0.01^3$	$0.05 \pm 0.01$
$\nu_e$ CC interaction	-	1	$1.14 \pm 0.11$	$1.08 \pm 0.10$
Total	16	1	$18.5 \pm 2.6$	$1.5 \pm 0.2$

**Table 1:** Comparison of the number of rejected events with the MC simulation.

on  $\nu_e$  identification efficiency for the ESD method comes from the track detection efficiency of HTS, differences with respect to the actual track reconstruction and shower detection procedure including the visual scan by a human, and the statistical uncertainty of the MC simulation. The breakdown is shown in Table 2. The fractional contribution of the ESD method with respect to the CSH method is 0.07/0.03, which is relatively smaller due to the sub-sample selection with the vertex film number. Taking account of the contribution, the overall systematic uncertainty has been estimated to be 19%/10%. The statistical uncertainties from the number of  $0\mu$  events used for the normalization are 3% and 10% for the CSH and ESD methods, however they are sufficiently smaller than the systematic uncertainty.

		< 10 GeV	$\geq$ 10 GeV
Flux, cross section and location		14%	6%
CSH identification		15%	8%
ESD identification	Track detection efficiency with HTS	15%	9%
	Difference of actual process with MC	4%	3%
	Statistical uncertainty in MC	20%	10%
	Overall in ESD identification	25%	14%
Overall		19%	10%

**Table 2:** The breakdown of the systematic uncertainties for the  $\nu_e$  detection efficiencies of the CSH and ESD methods.

The systematic uncertainties of the prompt  $\gamma$  conversion and hadron+ $\gamma$  random coincidence are strongly dominated by the statistical uncertainties of the MC simulation, because of extremely small sample sizes remaining after applying the background reduction methods. All other systematic uncertainties are negligible for those 2 background sources. For the  $\tau \rightarrow e$  decay, the uncertainties of  $\nu_\tau$  detection efficiency [2] and the ESD identification efficiency mentioned above are taken into account. Table 3 shows the breakdown of them for each background source together with those of the CSH method.

## References

- [1] N. Agafonova et al. (OPERA Collaboration), <https://arxiv.org/abs/2211.04636>
- [2] N. Agafonova et al. (OPERA Collaboration), Phys. Rev. Lett. 120, 211801 (2018).
- [3] N. Agafonova et al. (OPERA Collaboration), J. High Energy Phys. 06 (2018) 151.

CSH	prompt $\gamma$ conversion	100%
	hadron+ $\gamma$ random coincidence	negligible
	$\tau \rightarrow e$ decay	29%
ESD	prompt $\gamma$ conversion	58%
	hadron+ $\gamma$ random coincidence	100%
	$\tau \rightarrow e$ decay	22%
Overall		36%

**Table 3:** The breakdown of the systematic uncertainty for the background sources except the beam  $\nu_e$ .